Pediatric Electrocardiography

edited by
JEROME LIEBMAN, M.D.
ROBERT PLONSEY, Ph.D.
PAUL C. GILLETTE, M.D.

Pediatric Electrocardiography

edited by

JEROME LIEBMAN, M.D.
Professor of Pediatrics
Director, Pediatric Cardiology
Case Western Reserve University
Rainbow Babies & Childrens Hospital
Cleveland, Ohio

ROBERT PLONSEY, Ph.D.
Professor of Bioengineering
Director, Department of Bioengineering
Case Western Reserve University
Cleveland, Ohio

PAUL C. GILLETTE, M.D.
Professor of Pediatrics
Associate Professor of Experimental Medicine
The Lillie Frank Abercrombie Section of Pediatric Cardiology
Baylor College of Medicine and Texas Children's Hospital
Houston, Texas

Made in the United States of America

Dedication

To
Judy, Vivian and Sarah
and to
Joanne, Matt, Laura and Amy Liebman
Daniel Plonsey
Noelle and Cathy Gillette

Foreword

This is a comprehensive scholarly volume on pediatric cardiology that brings the discipline into the last quarter of the 20th Century.

There are two previous volumes on the subject produced by former trainees of the cardiology program at the Children's Hospital in Boston. Dr. Guntheroth's small book on pediatric electrocardiography was published in the mid sixties with the avowed goal of producing an approach to electrocardiography emphasizing pediatric experience. The approach was based on scalar tracings, interpreted vectorially. Dr. Ellison's monograph, published in the early seventies, focused entirely on congenital heart disease and utilized the Frank vectorcardiogram for estimating severity of specific cardiac malformations.

The scope of this book is much wider than that of either of the two referred to above. First of all, through collaboration with basic scientists, the physical principles underlying electrical phenomena are explained in depth and brought in continuously, into specific clinical situations. Secondly, hypertrophy, conduction abnormalities, as well as ST and T wave changes are being looked at not only in terms of standard electrocardiograms but also utilizing a variety of vectorial leads including the Frank and McFee systems. Thirdly, by recruiting as coauthors foremost practitioners of intracardiac electrophysiology in children, Dr. Liebman added another dimension to his volume—the up-to-date interpretation of pediatric arrhythmias.

At this time, it is essential to give a new intellectual stimulus to pediatric electrocardiography. Imaging, particularly in terms of two dimensional ultrasound, has made giant strides within the last decade. Noninvasive assessment of cardiac morphology already introduces pictures comparable to high grade angiograms, and the end of the development, through technical innovations, is not even in sight. By refocusing our attention on the electrical phenomena of the heart, by collecting all the up-to-date information in the field in one volume, giving the data an intellectual foundation in basic science and extending the scope into the burgeoning field of clinical electrophysiology, this book should stimulate renewed interest in pediatric electrocardiography.

By having this book on his shelf, the adult cardiologist will be able to better understand heart disease in infants and children, and the pediatric cardiologist's diagnostic armormentarium will be expanded by scientific electrocardiography over and beyond that offered by reading twelve lead tracings in terms of patterns. This volume should prove to be very helpful, not only to clinicians but also to students and fellows in cardiology, by stimulating research in the field.

Alexander S. Nadas, M.D.
Chief, Department of Cardiology
Professor or Pediatrics
Harvard Medical School

Preface

The field of pediatric electrocardiography, as reflected in this book, can be divided into three areas. The first, involving the basic science of electrocardiography, has been virtually ignored by most clinical electrocardiographers. Dr. Plonsey, one of a handful of theoretical electrocardiographers, has the knack of gradually bringing the very basic science into the realm of basic principles and then relating these principles to the practical problems of interpretation. Only when we truly understand the myocardial source, what happens to that source when it reaches the epicardium, and what then happens to the epicardial potentials before they reach the body torso, can we truly understand the electrocardiogram. In actual fact, it is perhaps not fair to state that most clinical electrocardiographers virtually ignore the basic science—for when arrhythmias are considered, the basic science is constantly being discussed and investigated, entering into our increasing knowledge in that area. Dr. Gillette, one of the leaders in the field of arrhythmias related to children, is one of those new breed of clinical electrocardiographers who is also constantly studying the related basic science. Dr. Garson, working with Dr. Gillette, and utilizing the new sophistication, has developed a very innovative approach to interpretation which should help the serious reader to be very practical and, at the same time, scientific.

As cardiologists have indeed become more and more sophisticated interpreters of arrhythmias, the field has stagnated as related to interpretation of hypertrophy, ventricular conduction defects, etc. In fact, the majority of readers appear to have felt that the problems of understanding the distortions between the myocardial source and the body surface are so great, that a "pattern" reading approach seems simpler and, in fact, as good as any other method. But we believe, helped by Dr. Plonsey and the remarkable though small cadre of other investigators in basic electrocardiography (particularly including Drs. Madison Spach and Roger Barr at Duke University, but many others, including Drs. Allen Scher, J. A. Abildskov and his group, the late Daniel Brody, Leo Horan, Nancy Flowers, and Bruno Taccardi) that a scientific approach to interpretation is not only possible, but also necessary. Such an approach is attempted in this book. Note that there is no true separation, when discussing interpretation of hypertrophy, etc., between standard electrocardiography and vectorcardiography. The principles are the same.

But even as I write this, it is with the expressed understanding that this book's approach will also soon be outdated, for the burgeoning field of body surface mapping is becoming increasingly exciting. Drs. Plonsey and I, working with Drs. Thomas and Rudy, are working with a 180 lead system. Meanwhile, Dr.. Abildskov's group, particularly Drs. Lux and Wyatt, have developed a limited lead body surface map system (32 leads), while Drs. Spach and Barr have also developed a limited lead body surface map system (24 leads). It may very well be, as Dr. Spach has frequently expressed, that a limited lead body surface potential map methodology may be the electrocardiogram of the future.

Finally, reverting back to an earlier chapter, Dr. Thomas has elegantly described the problems and science related to the measurement of electrocardiography on the body surface. It is quite clear that the majority of electrocardiograms taken in the world today are single channel, low-frequency response machines, which record variable and often spurious potentials. Analysis of his chapter should lead the readers to demand more of our electrocardiograph manufacturers, as well as demanding more of ourselves in our methods of recording.

There is not enough space to thank all those who helped prepare the manuscript in Houston's Division of Pediatric Cardiology and Case Western Reserve University's Department of Biomedical Engineering, but I would like to thank all those who have come through the Pediatric Cardiology Division of Rainbow Babies & Childrens Hospital over the past 20 years. I would like to particularly acknowledge the long-term help of Miss Louise Muth, who taught me how to take a proper electrocardiograph with an old Cambridge string galvanometer during my internship and who is still with us, demanding ever finer quality of our recordings—and our illustrations. I would also like to thank Mr. Angel Martinez for his excellent photography, and Miss Jacqueline Sinkford, secretary in the Pediatric Cardiology Division, for her years of devotion and for typing and putting together the final manuscripts during January's and February's cold Cleveland nights. A final acknowledgement must go to Dr. Yoram Rudy, one of the younger breed of theoretical electrocardiographers, who works with Dr. Plonsey, and unselfishly helped make sure that all of Dr. Plonsey's illustrations were perfectly drawn, after Dr. Plonsey left Case Western Reserve for a year's sabbatical with Drs. Spach and Barr at Duke.

Jerome Liebman, M.D.

Contributors

Arthur Garson, Jr., M.D.
Assistant Professor of Pediatrics and Medicine
Baylor College of Medicine
Associate in Pediatric Cardiology
The Lillie Frank Abercrombie Section of Pediatric Cardiology
Texas Childrens Hospital
Houston, Texas

Paul C. Gillette, M.D.
Professor of Pediatrics and Associate Professor of Experimental Medicine
The Lillie Frank Abercrombie Section of Pediatric Cardiology
Baylor College of Medicine and Texas Childrens Hospital
Houston, Texas

Jerome Liebman, M.D.
Director, Pediatric Cardiology
Rainbow Babies & Childrens Hospital
Cleveland, Ohio

Robert Plonsey, Ph.D.
Director, Dept. of Bioengineering
Case Western Reserve University
Cleveland, Ohio

Anthony Raviele, M.D.
Assistant Professor of Pediatrics
Dept. of Pediatric Cardiology
Emory University School of Medicine
Atlanta, Georgia

Cecil W. Thomas, Ph.D.
Dept. of Bioengineering
Case Western Reserve University
Cleveland, Ohio

Contents

The Biophysical Basis for Electrocardiology

1. INTRODUCTION

The goal of this chapter is to explain as simply as possible, but without sacrificing accuracy, the electrophysiological origins of the electrocardiogram. Enough is known about the system to make possible an explanation of electrocardiographic signals based upon the behavior of the single cell, intercellular activation, and the nature of the volume conductor. The outlook presented here is comprehensive and, to the extent possible, quantitative.

The heart behaves like an electrical generator, and because it lies in a conducting medium, currents are caused to flow within the entire torso. The electrocardiogram is simply a manifestation of the presence of these currents. One describes the capabilities of the heart to set in motion the current flow fields by defining *cardiac sources*. These sources are analogous to electrical batteries. Given their spatial and temporal distribution as well as a description of the volume conductor in which they lie permits the evaluation of the electrocardiographic potentials through the application of the laws of electricity.

To introduce the basic concepts of source and field we consider first several examples from electrostatic fields. In fact these examples will prove useful later on because while electrostatic and current flow fields (in which we are actually interested) are quite different physically, they obey similar relationships. The main reason for their introduction at this point, however, is because the approach we shall be using is more easily described using electrostatics.

Once the basic ideas of source and field have been discussed and the properties of the simple monopole and dipole electrostatic fields described, we shall consider their specific application to cardiac electrophysiology. We will be interested in a quantitative description of cardiac sources and will learn that this involves widely distributed dipoles (double layers) in general. We will also examine the approximate source representation of a single fixed position dipole, an approximation that underlies most of conventional electrocardiography.

We shall avoid the use of mathematics whenever possible, but frequently it summarizes concepts so succinctly that we shall break our rule for the increasing number of readers with mathematical training. In all cases we will provide a word description (but it may not be as good).

2. ELECTROSTATIC SOURCE AND FIELD: MONOPOLE

We are all familiar with the ability of a comb or other plastic object when rubbed to attract small bits of paper. If a glass rod is rubbed on a silk cloth both rod and cloth attract paper. We believe that the glass and cloth have become "electrified" in this process. Some readers will recall the experiment in their elementary physics laboratory where a small gilded pith ball suspended by a silk string is brought into contact with the glass rod. The gold "conducting" material apparently removes the electrification while the silk thread "insulates" the electrified ball. If two such suspended balls are electrified by the glass rod they demonstrate their electrification since they repel each other. If, however, one is electrified by contact with the silk cloth and the other by contact with the glass rod then they are found to attract each other. This simple experiment suggests the existence of two kinds of electricity, positive and negative, which normally neutralize each other; the rubbing process separates the two, with positive charge remaining on the glass rod and negative charge on the silk cloth. If, furthermore, we postulate that like charges repel while unlike charges attract, then the aforementioned experiments are accounted for.

By means of a torsion balance Coulomb in 1785 investigated the electrostatic force between two charged bodies whose sizes were small compared with their separation (in effect they were "point charges"). The result can be expressed by the following equation

$$\bar{F}_{ab} = Q_aQ_b/(4\pi\epsilon R^2)\bar{a}_R \qquad (1)$$

which reads that the force exerted by a charge of magnitude Q_a on a charge Q_b is proportional to their product and inversely proportional to the square of their separation R. The factor $4\pi\epsilon$ accounts for the units used and for the medium in which the charges lie (ϵ is the permittivity). The unit magnitude vector $\bar{a}_R$ is along a line connecting the two charges and away from Q_a so that if Q_a and Q_b have the same sign the force is one of repulsion but if of opposite sign it is an attractive force. If Q_a, Q_b are in coulombs, R in meters, and $\epsilon = 8.854 \times 11^{-12}$ farads/meter (permittivity of free space), then $\bar{F}$

is the force in newtons. We have placed bars over those quantities which are vectors to remind us of this fact. (Vectors, of course, have both direction and magnitude while scalars have magnitude only. Wind velocity exemplifies a vector and temperature a scalar.) In equation (1) $\bar{F}$ necessarily has the direction of $\bar{a}_R$ for the equality to be satisfied.

Coulomb's law as expressed in equation (1) regards the force exerted by Q_a on Q_b as acting through (across) the intervening medium. This formulation is described as an "action-at-a distance" law. The observed force arises as if Q_a could directly influence Q_b through the intervening space.

The same result can also be realized based on another principle known as the *field concept*. According to this view Q_a sets up a field which pervades all of space, while Q_b lying in that field is acted on the field. Thus the force exerted by Q_a on Q_b is communicated by means of this field. The force exerted by the field on Q_b depends on the strength of the field set up by Q_a. (However, the force exerted by a field does not depend on the origin of the field.) The field concept postulates the existence of a field set up by Q_a even though no charge Q_b is present to detect it.

The electrostatic field is defined as the force per unit charge. Since the force is a vector and charge a scalar the field is a vector in the direction of the force. From equation (1), for example, we have

$$\bar{E} = \bar{F}/Q_b = Q_a/(4\pi\epsilon R^2)\bar{a}_R \qquad (2)$$

and $\bar{E}$ is the electric field. From the definition it follows that the force exerted by an electric field on a point charge Q_b is simply the product of the field and the charge. That is, from equation (2),

$$\bar{F} = \bar{E}Q_b. \qquad (3)$$

Suppose Q_b is in the presence of three point charges Q_1, Q_2, Q_3. The force on Q_b may be found by *superposition*, that is, the force due to Q_1, Q_2, Q_3 would each be calculated separately (as if it alone existed) according to equation (1). The result in each case is a vector representing the force. The net force on Q_b is the *vector sum*. The parallelogram law of vector addition, illustrated in Fig. 1.1, must be used to obtain the resultant vector (force). Alternatively, following the field concept, one first sums the separate fields from Q_1, Q_2, Q_3. (Vector addition is also required in this case.) The force on Q_b is then found directly from application of equation (3), where in this case $\bar{E}$ is the resultant field (from Q_1, Q_2, Q_3). The charges Q_1, Q_2, Q_3 are the *sources* of the field.

The electrostatic field of a point charge of unit strength is given by the expression of equation (2) with $Q_a = 1$. This field of a point source is known as a *monopole* field. We have tried to suggest the character of this field in Fig 1.2 where we show that it is directed radially outward from the source location. The decreasing density of the field lines suggests a decrease in magnitude (which actually diminishes as $1/R^2$).

The force experienced by the point charge Q_b in the electrostatic field of Q_a is like that of a ball in the gravity field of the earth. (The force of attraction between the
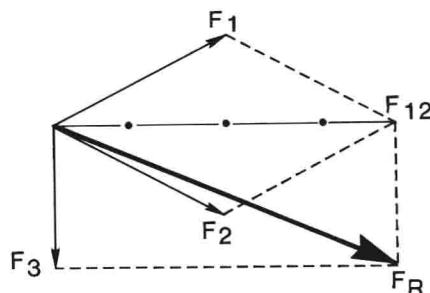

Figure 1.1 The force on Q_b from Q_1 is the vector $\bar{F}_1$. That due to Q_2 is $\bar{F}_2$, while that arising from $\bar{Q}_3$ is $\bar{F}_3$ (see text). The sum of $\bar{F}_1 + \bar{F}_2$ is found by the "parallelogram law." This requires that a parallelogram be formed with $\bar{F}_1$ and $\bar{F}_2$ as sides, the vector sum in the diagonal $\bar{F}_{12}$. The sum of $\bar{F}_3 + \bar{F}_{12}$ is found in the same way and is the resultant of $\bar{F}_1 + \bar{F}_2 + \bar{F}_3 = \bar{F}_R$. The order of summation is irrelevant so that if, say, $\bar{F}_2 + \bar{F}_3 = \bar{F}_{23}$, then $\bar{F}_R = \bar{F}_1 + \bar{F}_{23}$, etc.
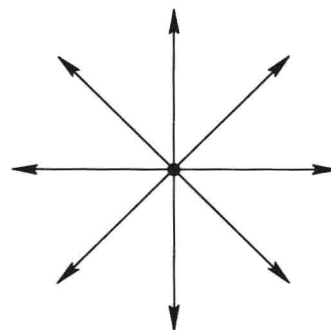

Figure 1.2 The electric field of a point charge is directed radially outward from the source. This is illustrated above. The decreasing density of the field is suggested by the diminishing density of flux (field) lines with increasing distance from the point source. Actually $|E| \propto 1/R^2$.

two bodies (earth and ball) is considered to result from a gravitational field established by the earth which, in turn, causes a force to be exerted on the ball). Because of the gravitational force, energy is required to raise the ball from, say, the floor to the table. According to the law of conservation of energy the work done in raising the ball appears in the form of *potential energy*. The ball on the table, like weights of a clock that have been raised, is capable of doing work—the higher the ball the greater the potential energy. In the same way the closer Q_b is moved to Q_a the more work that is required because of the opposing force, and hence the higher potential energy. Since the increase in potential energy (or simply *potential*) is the product of the force times the distance, then it follows that the force must be the rate of change of potential. (More precisely, the potential of energy is the integral of the force through a distance while the force is the *gradient* of the potential.) For the monopole field the potential is expressed in volts, V, and we have

$$\bar{E} = -\text{gradient } V \qquad (4)$$

or, in vector analysis notation

$$\bar{E} = -\nabla V \qquad (5)$$

In words equation (5) states that the electric field is given by the maximum rate of decrease (in view of the minus sign) of the electrical potential and has the direction of the maximum rate of decrease. A ball placed on the side of a (smooth) hill will roll in the direction of the gradient (maximum steepness). When E depends only on R, as for the monopole field described by equation (2), then (5) simplifies to

$$\bar{E} = -dV/dR \; \bar{a}_R, \qquad (6)$$

and we can infer from this that the electrical potential must be

$$V = Q_a/(4\pi\epsilon R). \qquad (7)$$

In practice the instruments we use measure only the difference in potential between two points in an electric field rather than the field directly. Usually one point is a specially chosen reference, often designated zero, so the other point is a specially chosen reference, often designated zero, so the other point is simply expressed in volts (or millivolts) and is *the* potential of that point. In electrocardiography, of course, we measure potential differences at the surface of the torso. But, like the tip of an iceberg, this is the surface manifestation of a *potential field* V (which has values everywhere in the body) and from which the electric field is related by equation (4). From an examination of equation (2) and equation (4) we note that the electric field can be expressed in newtons/coulomb or in volts/meter, both units being fully equivalent.

3. DIPOLE FIELDS, REFERENCE POTENTIAL

The field due to two point sources of equal magnitude but of opposite sign, when their separation is very small, is known as a *dipole field*. While such a source is nothing more than an example of two point sources, and therefore already considered (at least in principle) in the previous section, we shall see that it represents an important elementary source in its own right in electrocardiography. The field arising from a dipole can of course be determined by applying the principle of superposition; that is, equation (7) (or equation (2)) is separately applied to each point-source and the result summed. For the case where the positive source has the magnitude Q and lies on the z axis a distance d/2 from the origin and the negative point source (strength −Q) lies on the z axis but at −d/2 (this is illustrated in Figure 1.3), then application of equation (7) leads to an infinite series in terms involving increasing even powers of (d/R), namely

$$V = Qd \cos\theta[1 - (3/2 - 5\cos^2\theta/2)d^2/R^2 + \ldots]/(4\pi\epsilon R^2). \qquad (8)$$

For d/R ≪ 1 all but the first term can be neglected, and the first term alone is the true dipole field. The mathematical dipole in fact, requires that d → 0. Physical dipoles imply, usually, that d ≪ R, so that the leading term in equation (8) is a good approximation (the goodness depends on d/R being small). The product of charge magnitude Q and separation d is known as the *dipole*
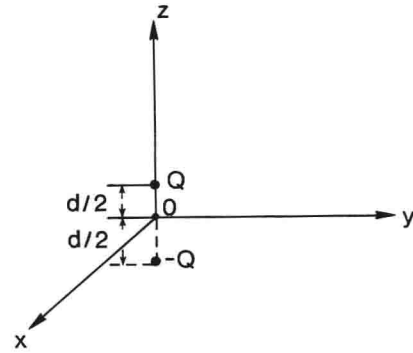

Figure 1.3 A dipole source is shown. This is an axial dipole directed along the positive z-axis. Its strength, M = Qd.

moment. We shall assign the symbol M = Qd, in which case

$$V = M \cos\theta/(4\pi\epsilon R^2). \qquad (9)$$

The dipole is viewed as being oriented from the negative to the positive source; in this case it is directed along the positive z axis. Compared with equation (7) which describes the monopole potential field to diminish as (1/R) we see that the potential field of the dipole, as expressed by equation (9), diminishes more quickly (as 1/R²). In fact the dipole electric field (one must take the gradient of V) will be found to diminish as 1/R³. The more rapid decrease of dipole relative to monopole arises because much of the field of the +Q source is offset by the nearby −Q source. Another feature of the dipole field is the angular dependence. Since cosθ is positive for 0 < θ < 90 the hemisphere in the direction of the dipole has positive potentials, while the hemisphere "behind" the dipole (i.e., 90 < θ < 180) is negative. The plane which is the perpendicular bisector of the dipole (in the example under consideration this is the XY plane) is at zero potential. A complete isopotential plot in a plane containing the dipole is given in Fig. 1.4 along with the associated electric field. Since the electric field corresponds to the potential gradient the former will be orthogonal to the isopotentials.

If the source consists of, say, three dipoles M_1, M_2, M_3 with arbitrary location and arbitrary orientation then the potential field due to all three can be found by superposition. We could, in principle, first choose the coordinate axis to be located at M_1 with the z axis in the direction of this dipole. Then the field at some particular location (θ_0, R_0) can be found from equation (9). The procedure could then be repeated for M_2 and M_3 and the potentials summed. (The process is complicated by the fact that a different coordinate system has been defined for each dipole.) For those versatile in vector calculus it is simpler to convert (9) into a form where both the location and orientation of each dipole source is arbitrary, but the coordinate axis is fixed (rather than having to be redefined for each dipole). Assuming the source at (x',y',z'), the field point of interest to be (x,y,z), and the dipole moment (relative to the fixed coordinate system) given by M (the vector direction is from the −Q
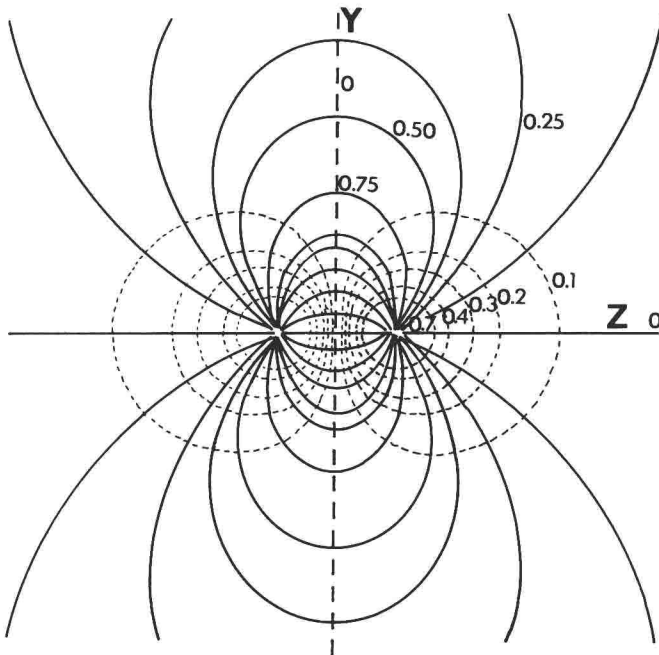
Figure 1.4 The field of the axial dipole in Fig. 1.3 is shown. The *solid lines* represent the electric field, while the *dotted lines* are isopotentials. The two sets of curves are mutually orthogonal.

to +Q) then

$$V = \overline{M} \cdot \bar{a}_R/(4\pi\epsilon R^2) \qquad (10)$$

where $R^2 = (x - x')^2 + (y - y')^2 + (z - z')^2$, $\bar{a}_R$ is a unit vector from the source point to the field point, and $M \cdot \bar{a}_R$ (the dot product) equals the magnitude of M times the cosine of the angle between M and $\bar{a}_R$. In the case where M is along the z axis and $(x', y', z') = (0, 0, 0)$, then $M \cdot \bar{a}_R = M \cos \theta$, so that equation (10) reduces to equation (9). For a distribution of dipoles $i = 1, 2, 3, \ldots,$ N then, by superposition, (11) can be written

$$V = \Sigma \overline{M}_i \cdot \bar{a}_{Ri}/(4\pi\epsilon R_i^2) \qquad (11)$$

where $R_i^2 = (x - x_i') + (y - y_i')^2 + (z - z_i')^2$, (x_i', y_i', z_i') being the location of the ith dipole M_i.

The potential field of equation (7) was found by integration of equation (2) with respect to R, and we arbitrarily took the constant of integration to be zero. That is, a constant could be added to equation (7) without affecting its correctness. We can see this by supposing that a constant C were added, in which case

$$V = Q_a/(4\pi\epsilon R) + C \qquad (12)$$

But the difference in potential between any two points (say at R_1 and R_2) is then

$$V_1 - V_2 = [Q_a(4\pi\epsilon R_1) + C] - [Q_a(4\pi\epsilon R_2) + C] \qquad (13)$$

and the result is independent of C (since it cancels out). Since physical measurement always deals with differences in potential, "absolute" potential doesn't exist. However, we frequently choose the zero reference such that C equals to zero in equation (12), in which case

equations (9) to (11) are as shown. In electrocardiography the reference potential is usually chosen to be the *Wilson central terminal*, about which more will be said later.

---

4. CURRENT FLOW FIELDS: SINGLE FIBER

In the science of electrostatics the sources are charges, the medium in which they lie is dielectrics (insulators), and the field produced is electric (electrostatic). The point charges are measured in coulombs, the medium is defined by a dielectric permittivity, ϵ, and the electric field is in volts/meter. In the study of the electrocardiogram the medium is a conductor (volume conductor) defined by a conductivity, σ. There is an electric field as in electrostatics, but because of the finite conductivity there is also a current. In fact since Ohms law must be satisfied the current density, $\bar{J}$, is given by

$$\bar{J} = \sigma\bar{E}. \qquad (14)$$

It turns out that electrophysiological sources are always dipolar in nature, although, generally, the dipoles are *distributed* over a surface or throughout a volume rather than being discrete. In electrostatics dipole sources once set up would remain in place, as would their fields (ad infinitum). In current-flow fields a dipole current source must continually supply energy to maintain the field it sets up. (The energy is reflected in Joule heating due to current flow through a resistive medium.) Apart from this requirement a current dipole in a uniform conducting medium sets up the same type of field as an electrostatic dipole in a uniform dielectric medium. Thus, if in Fig. 1.3 we replace +Q by a point current source +I and −Q by −I (one could actually create such a condition with an electric battery, since it is capable of supplying +I and collecting −I for a period of time), and if we designate the current dipole as P = Id, then the appropriate expression for the (electric) potential field V (corresponding to equation (9) is

$$V = P \cos \theta/(4\pi\sigma R^2) \qquad (15)$$

where σ replaces ϵ, and P replaces M. In a similar way equation (11) which applies to electrostatic fields transforms to

$$V = \bar{P} \cdot \bar{a}_R/(4\pi\sigma R^2) \qquad (16)$$

which applies to current flow fields. The field plot in Fig. 1.4 generated from equation (9) represents equation (15) equally well; the solid lines in that figure can be interpreted both as the electric field and the current density in view of equation (14).

How current flow sources arise in excitable tissue can be explained through the use of a simple example, that of the single active cell. Because of low resistance end-to-end coupling of cardiac cells (to be described in detail later) its functional behavior is similar to the very long fibers of striated muscle. Consequently the long single fiber is an appropriate choice both as a simple example of the excitatory process and as a representative (elemental) cell for cardiac muscle.

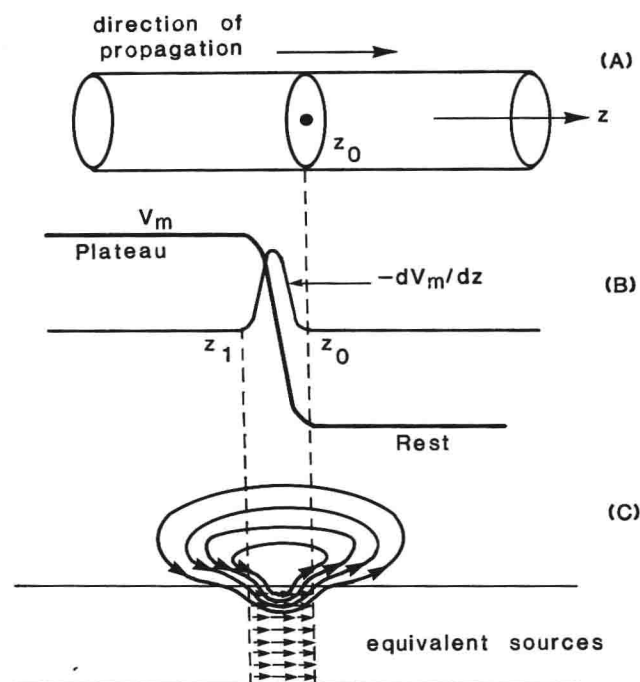In Fig. 1.5*A* we show a single cylindrical fiber on

Figure 1.5 (A) A single cylindrical fiber is shown oriented along the z-axis carrying an action potential propagating in the +z direction. (B) The spatial transmembrane potential V_m and $-dV_m/dz$ are shown; these represent conditions on the fiber depicted in (A). (C) The equivalent sources are an axial dipole density whose strength is proportional to $-dV_m/dz$. Some current flow lines are approximately shown.

which an action potential is propagating. The action potential has reached the point z_0, and the corresponding transmembrane potential is shown in Fig. 1.5B. Note that in the region ahead of the activation (i.e., $z \geq z_0$) the transmembrane potential is at rest. The point z_1 corresponds to complete depolarization, while the flat plateau is reflective of an idealized cardiac action potential. The depicted spatial action potential is derived from the temporal action potential through an assumed uniform velocity of propagation.

The changing transmembrane potential in the region from z_1 to z_0 causes a flow of current which links the intracellular with the extracellular medium. (Some flow lines are shown in Fig. 1.5C.; the outflow is the excitatory depolarization while the inflow corresponds to the triggering of the sodium mechanism which results in an elevated sodium conductance and consequent sodium influx.) These *action currents* correspond precisely to the current flow field of interest. Although the phenomena is time varying, its variation is slow enough so that it can be considered by static theory (steady current or an electrostatic analog) at each instant. In particular, the extracellular current and concomitant electric field (through equation (14)) or electrical potential (through equation (5)) behave as if they were generated by the dipole sources depicted in Fig. 1.5C. These sources are volume distributed axial dipoles lying in (filling) the axoplasm and having an axial strength (a volume density) proportional to the (spatial) rate of change of V_m

(this is described by $-dV_m/dz$). Consequently the dipole source is confined to the region z_1 to z_0, since elsewhere V_m is constant (unchanging). The dipole strength (density) is proportional to the quantity $-dV_m/dz$; hence, as shown in Fig. 1.5B; it rises from zero to a peak in the center and back to zero. For a field point at a sufficient distance this distributed dipole density source "looks like" a single dipole and the field generated, as a function of time, is that of a single z-oriented dipole propagating along the z axis at the velocity of propagation of the action potential.

5. INTRODUCTION TO CARDIAC ELECTROPHYSIOLOGY

The details of the process of cardiac activation are described in Chapter 3. For the ventricles, once excitation in the working musculature is initiated by the Purkinje system, its spread takes place through cell-to-cell conduction, grossly characterized as from endocardium to epicardium and from apex to base. In Fig. 1.6 we illustrate the results from an experiment for a perfused human heart; shown are activation surfaces at successive instants of time. Each isochronous surface (isochrone) represents the deepest penetration of activity and separates the resting tissue (ahead of the isochrone) from the active tissue (behind the isochrone).

One notes in Fig. 1.6 that isochronous surfaces lie, roughly parallel to the endocardial and epicardial surfaces. This is typical of the experimental results reported by many investigators. It may seem strange to point out that the cardiac fiber direction is also parallel to the endo- and epicardium, since this means that activation proceeds across the fibers. However, it turns out that activation is rapid along the fiber axis and slow across it, so that we observe, essentially, only the slow component.

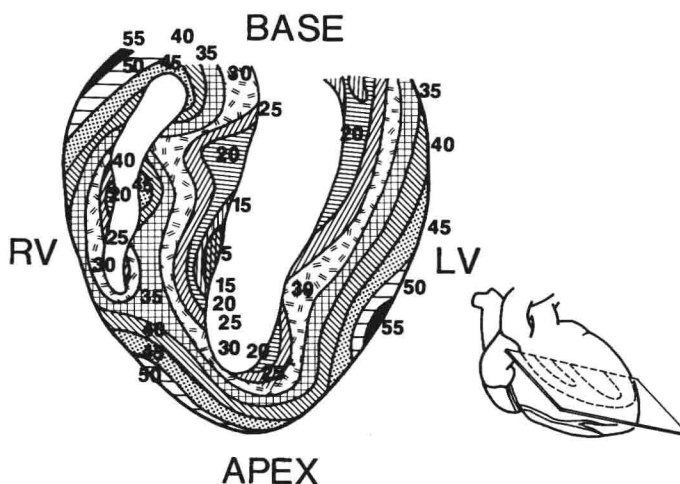One might wonder how conduction across the cardiac

Figure 1.6 Isochronous lines of activation of the human heart. Numbers refer to time in milliseconds where the zero reference corresponds to the first appearance of ventricular activity. (From D. Durrer et al.: *Circulation*, 41:899, 1970. Reproduced by permission of the American Heart Assoc., Inc.)

fibers can take place at all. While the details are not known with certainty it apparently involves low resistance end-to-end cellular connections which permit propagation along the fiber axis (as we've already noted), while, in view of the extensive anastomosing of the cells, such activation reaches lateral cells as well. This extensive interconnection of cardiac cells accounts for the description of the heart as a *functional syncytium.*

From a functional standpoint, and to the extent that successive isochrones reflect uniform propagation from endocardium to epicardium, we have depicted in Fig. 1.7A a portion of the free wall as if fibers were, in fact, oriented from endo-to epicardium. Such an idealized model will permit an evaluation of sources without the complication of accounting for the effects of the histology. For distant field points, such as the torso surface, the simplifying assumptions should prove generally satisfactory.

The *dotted line* in Fig. 1.7A depicts an isochrone at an instant of time. We show, in Fig. 1.7B, the spatial transmembrane action potential in each of the parallel fibers of Fig. 1.7A at that moment. This was constructed from a typical intracellular cardiac action potential (recorded vs. time) and an assumed uniform propagation from endo- to epicardium. Since the rising phase is normally around 1 msec in duration and the velocity around 50 cm/sec, the spatial extent of the rising phase, depicted in Fig. 1.7B, corresponds to around 0.5mm—or perhaps 1/20 the free wall thickness. Reference to Fig. 1.6 shows that this is a highly idealized, but not absurd, model. Note that the isochrone is located at the site of transition from resting to active tissue. The other dotted surface in Fig. 1.7A is at the interface between active and (idealized)
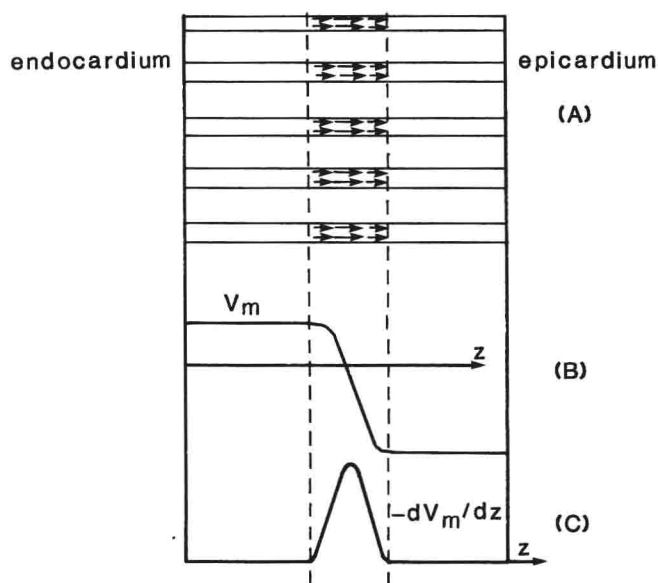
plateau tissue. This can be confirmed by reference to Fig. 1.7B.

Since each fiber in Fig. 1.7A is propagating an action potential of the form given in Fig. 1.7B, then the equivalent source can be found by application of the results obtained in Fig. 1.5. That is, each fiber contains an axial volume dipole distribution whose strength (density) is proportional to the rate of change of V_m in the z direction (i.e., $-\partial V_m/\partial z$). The density function is described in Fig. 1.7C (similar to Fig. 1.5C, of course), and the dipole distribution is sketched in Fig. 1.7A. No dipoles arise in the interstitial space, but since this occupies only around 20% of the volume, an effective uniform layer of dipoles lies behind each isochrone. In fact since the thickness of the dipole lamina is small compared to its extent (in general) it is usually considered as if it were infinitely thin and the dipole source thought of as comprising a surface density (rather than volume density). In this sense it constitutes what is known as a *double layer,* a mathematical phrase for a surface distribution of mathematical dipoles. (The source strength has the dimensions of dipole moment per unit area.) Henceforth we will use the simplified representation of the double layer in discussing cardiac sources but recognize that it is an approximation to the actual thick dipole layer.

We have stated that the dipole source strength is proportional to the axial rate of change of transmembrane potential ($-dV_m/dz$). The constant of proportionality depends on the direction of propagation relative to the actual fiber axis and consequently is not the same everywhere. Frequently this variation is neglected, and the double layer is assumed everywhere uniform in strength.

During recovery there will be a spatial distribution of V_m and sources will, as before, depend on the rate of change of V_m (not only with respect to z but possibly x and y as well). We shall return to this later in our discussion of the origins of the T wave. Suffice it to note, at this point, that recovery is not a propagated process, so the determination of the spatial distribution of V_m is much more complicated than the propagation phenomena that permits modeling the activation process (e.g., Fig. 1.7).

From a functional standpoint each cardiac cell behaves as if it were contiguous with each of its neighbors. This reflects the observation that an ectopic stimulus introduced at any intramural site results in a closed outward propagating wave (i.e., spreading uniformly). Consequently, the heart is considered to be an electrical syncytium; that is, it behaves as if it were like a single interconnected cell. We have seen how for a single fiber (essentially a one dimensional excitable system) the dipole moment density is related to the spatial rate of change of V_m (i.e., $-dV_m/dz$). Since the cardiac muscle syncytium is a three dimensional cellular structure one can have variations of V_m in all (i.e, x,y, and z) directions. Consequently dipole sources can be established with components in the z direction proportional to $-dV_m dz$ and also with x components proportional to $-dV_m/dx$ as well as y components proportional to $-dV_m/dy$. Those familiar with vector analysis will recognize that all of

Figure 1.7 (*A*) Hypothetical fiber orientation from endo- to epicardium to account for propagation in this direction. (*B*) Spatial transmembrane potential on each fiber in (*A*). (*C*) The function $-dV_m/dz$ is plotted. The dipole source density is proportional to this result. Dipole sources are depicted in (*A*) and lie within each fiber.

this is equivalent to establishing the total dipole moment density as proportional to $-\nabla V_m$.

6. CARDIAC SOURCES

Fig. 1.8 shows the measured isochrone and potential field distribution in a canine heart at 17 and 24 msec.[1] The sources at this moment, applying knowledge derived from section 5 above are double layers lying just behind all isochrones. (The isochrones are shown dotted with arrows to indicate the direction of propagation.) If each double layer were subdivided into many small area elements then each element of double layer can be treated like a single dipole, and the total field can be found by summing the dipole field from each. This exact procedure reflects both the shape, extent, and magnitude of the double layer. When the double layer is uniform (an assumption frequently made) then its field can be expressed by its *solid angle*. The solid angle is defined by the lines drawn from the field point to the periphery of the double layer and is proportional to the degree of opening of the cone which is thus formed. (A more precise definition will be given section 9 below.) A rough idea of the field can be found by replacing each activation double layer by a single dipole. (This approximation is a crude one unless the extent of the double layer is smaller than the distance to the field point.) The opti-

mum single dipole approximation can be deduced when the double layer periphery is essentially planar. A planar double layer generates the same field as the actual one if both have the same periphery, since both have the same solid angle. The planar double layer is best approximated by a single dipole which is perpendicular to the plane at its "center of gravity" and whose magnitude is proportional to the planar area. If a sufficiently accurate calculation of the double layer fields in Fig. 1.8 was performed then the result would correspond to the measured potential fields. (Positive potential areas are stippled and negative areas cross-hatched.)

To give some additional insight into double layer fields, in Fig. 1.9 we show a double layer in the form of a large circular disc along with the potential and electric field it generates. The latter fields were obtained, as suggested above, by summing the dipole contribution from a large number of component area elements. It is not surprising that the region ahead of the double layer is one of positive potential while the region behind the double layer is negative; this corresponds to the potential generating character of each isolated dipole element which constitutes the double layer disc (Equation (4) is utilized in this computation). At a very large distance (not shown too well in Fig. 1.9) the field behaves similar to that of a single dipole perpendicular to the disc at its center. Close to the double layer the potential falls off
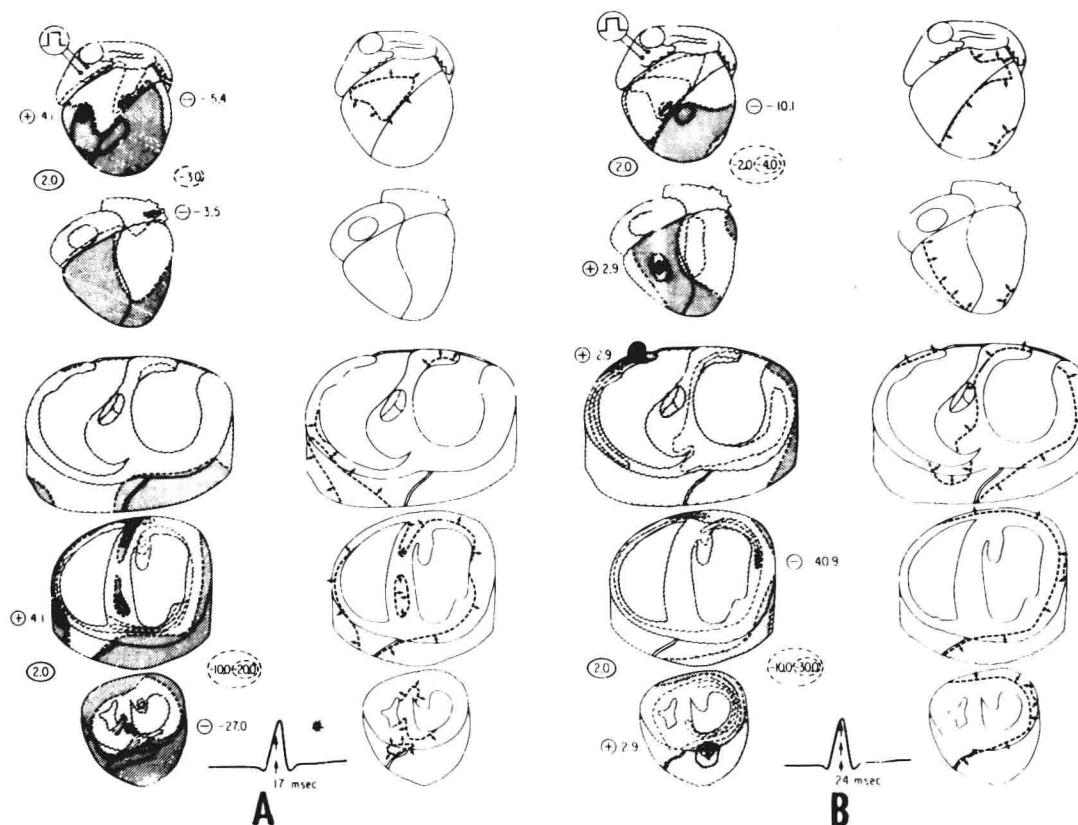

Figure 1.8 (*A*) The potential distribution on the surface and over three cross-sections of a canine heart is shown in the left column for 17 msec following normal activation. Positive areas are *stippled* and negative areas *cross-hatched*. For the same instant the right hand column shows the position of all activation isochrones. The direction of propagation of isochrones is shown by the *arrows*. (*B*) Same as (*A*) but at 24 msec. (Reproduced by permission of the American Heart Assoc., Inc.[1])
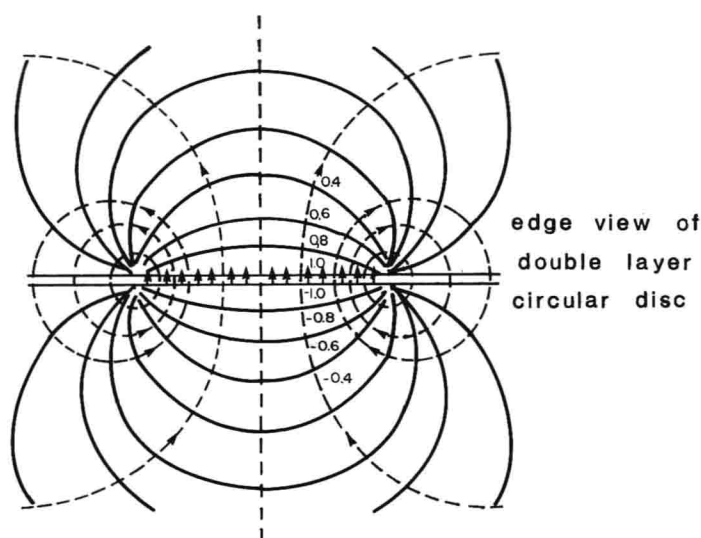
edge view of
double layer
circular disc

Figure 1.9 The potential and electric field from a circular disc current double layer. The current flow field is proportional to the electric field.

uniformly, and the electric field is directed away from the positive side and toward the negative surface. There is a relatively large drop in potential in crossing the double-layer so that the demarcation of positive and negative potential regions is sharp, particularly along the double layer itself. We also see this reflected in Fig. 1.8, where in most instances the ischochrone (hence double layer) is associated with the demarcation of positive and negative potentials. Exceptions can occur when a second nearby source produces a potential field which is sufficiently large to "overwhelm" the local effects of a particular double layer. Such exceptions can be found in Fig. 1.8.

Fig. 1.8 illustrates the complexity of a normal activation pattern. At 17 msec we noted a collapsing (colliding) wave in the septum. At 24 msec, there are residual patches of activation in the right ventricle and a *double envelopment* of the left ventricle. The double layer sources are consequently complex in form and distributed throughout the heart.

If we view an approaching car at night it appears at first to have a single headlight and only when it comes closer can the separate sources of light be resolved. In the same way each complex double layer source of cardiac activation (as illustrated in Fig. 1.8) appears as a single dipole to a distant "viewer." The single dipole is simply the vector sum of all dipole elements that constitute the double layer as if all such dipoles had a common origin. Thus by neglecting the dipole element distribution a vector addition can be performed, and a net dipole, representing the total double layer source, can be obtained. The same point was made in describing the field of the double layer disc shown in Fig. 1.9 as essentially that of a single dipole, provided the distance to the field is large compared to the radius of the disc—say five times the radius or greater. The field near the disc is considerably different from that near a single dipole, as is clear by comparing Fig. 1.9 and Fig. 1.4.

When activation of the heart is just starting only a single small isochrone may be present, and the single dipole approximation to it will be well justified. In the early activity several isochrones in close proximity in the septum and anterior portions of the heart may exist. Since each double layer is small a single dipole can approximate each, and the source will then be well represented by distribution of discrete dipoles. If, furthermore, the extent of the dipole distribution is small compared to the distance to the field then they can be summed (vectorially) as if at a common origin (i.e., neglecting their actual separation) and a single resultant obtained. Under these conditions we speak of the heart behaving dipolarly and can think of the entire heart as being represented by a single dipole.

Clearly there are times during cardiac activation when right and left ventricular activation are widely separated, and/or when each activation isochrone is itself extensive, where it is poorly justified to simply add up dipole elements disregarding their geometrical arrangement. Suppose, for example, that the approximating rightward activation dipole (right ventricle) and leftward dipole (left ventricle) were equal and opposite. A net zero resultant vector is then obtained while it is clear that fields are being generated by the source distribution. (A mechanical analogy is one where an upward force is applied to one propeller tip and an equal downward force at the other; while the vector forces "cancel" it is clear that the propeller is not in equilibrium.) In spite of all these considerations the resultant vector sum of all activation dipole elements is of central interest in conventional electrocardiography. This quantity is defined as the *heart dipole* or *heart vector* and normally viewed as fully representing the electrical sources of the heart. It is clearly an approximation, sometimes surprisingly good, but often inadequate. The limitation arises because substantial nondipolar behavior is observed in both normal and abnormal electrocardiography.

The heart vector will have a different magnitude and direction at each instant of time reflecting the changing shape and extent of isochronal double layers which contributes to it. Since the underlying electrophysiological process is uniform and continuous, the locus of the tip of the heart vector at successive instants of cardiac activation and recovery is a smooth curve in space. This curve is called the *vector loop*. Vectorcardiography is based on lead systems which are specifically designed to disregard the spatial distribution of double layer sources, and consequently to measure the vector loop itself. (Further details will be provided in the following chapters.) In this case the vector loop represents the totality of electrical information concerning the heart and clearly overlooks whatever information might be associated with the particular distribution of cardiac sources.

Since the distance from the anterior torso surface to the heart is usually the same order of magnitude as the extent of the sources within the heart, body surface potentials (contrary to the dipole hypothesis) will be sensitive to the spatial configuration of the underlying double-layer sources. Studies have clearly demonstrated that nondipolar contributions are not negligible. As a